Title

Evidence that Clostridium perfringens Enterotoxin-Induced Intestinal Damage and Enterotoxemic Death in Mice Can Occur Independently of Intestinal Caspase-3 Activation

Journal

Infection and Immunity, 86(7)

ISSN

0019-9567

Authors

Freedman, John C
Navarro, Mauricio A
Morrell, Eleonora
et al.

Publication Date

2018-07-01

DOI

10.1128/iai.00931-17

Peer reviewed

AMERICAN SOCIETY FOR MICROBIOLOGY | Infection and Immunity®

HOST RESPONSE AND INFLAMMATION

Evidence that *Clostridium perfringens* Enterotoxin-Induced Intestinal Damage and Enterotoxemic Death in Mice Can Occur Independently of Intestinal Caspase-3 Activation

John C. Freedman,[a] Mauricio A. Navarro,[b] Eleonora Morrell,[b] Juliann Beingesser,[b] Archana Shrestha,[a] Bruce A. McClane,[a] Francisco A. Uzal[b]

[a]Department of Microbiology and Molecular Genetics, University of Pittsburgh School of Medicine, Pittsburgh, Pennsylvania, USA

[b]California Animal Health and Food Safety Laboratory, San Bernardino Branch, School of Veterinary Medicine, University of California—Davis, San Bernardino, California, USA

ABSTRACT *Clostridium perfringens* enterotoxin (CPE) is responsible for the gastrointestinal symptoms of *C. perfringens* type A food poisoning and some cases of nonfoodborne gastrointestinal diseases, such as antibiotic-associated diarrhea. In the presence of certain predisposing medical conditions, this toxin can also be absorbed from the intestines to cause enterotoxemic death. CPE action *in vivo* involves intestinal damage, which begins at the villus tips. The cause of this CPE-induced intestinal damage is unknown, but CPE can induce caspase-3-mediated apoptosis in cultured enterocyte-like Caco-2 cells. Therefore, the current study evaluated whether CPE activates caspase-3 in the intestines and, if so, whether this effect is required for the development of intestinal tissue damage or enterotoxemic lethality. Using a mouse ligated small intestinal loop model, CPE was shown to cause intestinal caspase-3 activation in a dose- and time-dependent manner. Most of this caspase-3 activation occurred in epithelial cells shed from villus tips. However, CPE-induced caspase-3 activation occurred after the onset of tissue damage. Furthermore, inhibition of intestinal caspase-3 activity did not affect the onset of intestinal tissue damage. Similarly, inhibition of intestinal caspase-3 activity did not reduce CPE-induced enterotoxemic lethality in these mice. Collectively, these results demonstrate that caspase-3 activation occurs in the CPE-treated intestine but that this effect is not necessary for the development of CPE-induced intestinal tissue damage or enterotoxemic lethality.

KEYWORDS *Clostridium perfringens*, enterotoxin, caspase-3, intestinal damage, enterotoxemia

Clostridium perfringens enterotoxin, or CPE, is the primary virulence determinant when *C. perfringens* type A strains cause food poisoning and non-foodborne human gastrointestinal diseases such as antibiotic-associated diarrhea (AAD) (1). CPE-producing type A strains are responsible for approximately 1,000,000 cases of food poisoning/year in the United States and ~5 to 10% of all AAD cases (1, 2). Tragically, CPE-producing *C. perfringens* strains have also been implicated during the past decade in several severe food poisoning outbreaks involving fatalities in U.S. psychiatric institutions (3, 4). The severity of these outbreaks likely involved predisposing medical conditions that facilitated absorption of CPE from the intestines to cause a lethal enterotoxemia (3, 4, 5).

CPE is produced by *C. perfringens* only during the process of sporulation (6). After completion of sporulation and lysis of the mother cell in the intestines, CPE is released into the lumen (6). CPE then binds to exposed claudin receptors on the surface of cells at the apical tips of intestinal villi (6, 7). Once receptor bound, CPE oligomerizes into a

Received 18 December 2017 **Returned for modification** 14 January 2018 **Accepted** 15 April 2018

Accepted manuscript posted online 23 April 2018

Citation Freedman JC, Navarro MA, Morrell E, Beingesser J, Shrestha A, McClane BA, Uzal FA. 2018. Evidence that *Clostridium perfringens* enterotoxin-induced intestinal damage and enterotoxemic death in mice can occur independently of intestinal caspase-3 activation. Infect Immun 86:e00931-17. https://doi.org/10.1128/IAI.00931-17.

Editor Vincent B. Young, University of Michigan-Ann Arbor

Address correspondence to Francisco A. Uzal, fuzal@cahfs.ucdavis.edu.

J.C.F. and M.A.N. contributed equally to this article.

hexameric prepore; each CPE in the prepore then extends a β-hairpin loop to form a β-barrel that inserts into the membrane to form an active pore (8, 9). Previous *in vitro* studies using Caco-2 cells demonstrated that this CPE pore causes a Ca^{2+} influx into cells and a K^+ efflux from cells (10, 11).

In Caco-2 cells, the Ca^{2+} influx triggers calpain and calmodulin activation, which, in turn, can activate two distinct downstream cell death pathways, i.e., apoptosis and oncosis/necrosis (12). With a low *in vitro* CPE dose, caspase-3 activation becomes robust in toxin-treated Caco-2 cells. However, this effect was not observed when Caco-2 cells were treated with a high *in vitro* CPE dose, which resulted in cells dying instead by oncosis (13). When an inhibitor of caspase-3 activation was used to pretreat Caco-2 cells prior to a low-dose CPE treatment, the cells were protected from CPE-induced cell death (13). In contrast, protection from high CPE doses was not afforded by pretreatment with the same caspase-3 inhibitor. Instead, cytotoxicity was delayed in Caco-2 cells treated with a high CPE dose if glycine, an inhibitor of oncosis, was present (13). Taken together, these seminal studies demonstrated that Caco-2 cells respond in a dose-dependent manner to CPE challenge by entering either caspase-3-mediated apoptosis (at a low CPE dose) or oncosis/necrosis (at a high CPE dose).

While the previous *in vitro* studies identified important aspects of CPE-induced cell death *in vitro*, their relevance to CPE-mediated disease is not clear. In some aspects, Caco-2 cells resemble the enterocytes that line the small intestine; e.g., they can form tight junctions and brush border membranes (14). However, Caco-2 cells have a cancerous origin, produce limited amounts of mucus, and do not reflect the heterogeneity of cell types observed in the mammalian intestine, which include enterocytes, goblet cells, enteroendocrine cells, Paneth cells, and M cells (15–17). Another difference between the *in vitro* growth of Caco-2 cells as monolayers on plastic surfaces versus intestinal cells *in vivo* is that Caco-2 cells uniformly produce abundant amounts of accessible claudin CPE receptors, such as claudin-4 (9). This phenotype is not observed *in vivo*, where the majority of exposed claudin-4 is present on cells located at the villus tips (18). This finding was corroborated by immunohistochemistry studies showing that CPE predominantly binds at the villus tips in the rabbit small intestines (18).

Also notable is the *in vivo* observation that, while CPE binds primarily to the villus tips in the small intestine, this toxin destroys the entire small intestinal villus (18, 19). A possible insight into this phenomenon was provided by a recent study demonstrating that, *in vitro*, CPE-insensitive rat fibroblast cells are killed by supernatants from cultures of CPE-treated sensitive cells (20). A host serine protease appears to mediate this bystander killing. Death of the supernatant-treated fibroblasts also required caspase-3 activation in both the fibroblasts and in the CPE-treated sensitive cells (20).

Collectively, the *in vitro* findings suggest that, at some concentrations, CPE may bind to and damage intestinal villi by processes involving caspase 3 activation. To test this hypothesis, the current study utilized a murine ligated small intestinal loop model of CPE-induced disease (5). This model offers several distinct advantages over other ligated intestinal loop models, including the following: (i) the abundance of reagents available for murine studies is far greater than that for other animal models, (ii) mice treated with CPE are sensitive to CPE-induced death by enterotoxemia (5), and (iii) much more is known about the *in vivo* mechanisms of cellular death in small rodents than in other animal models. Using this model, the current study investigated whether CPE treatment activates caspase-3 and, if so, whether this effect is required for CPE-induced intestinal damage.

RESULTS

CPE activates caspase-3 in the mammalian small intestine in a dose-dependent manner. CPE-induced intestinal damage is considered necessary for this enterotoxin to cause fluid and electrolyte loss in the intestine (18). CPE-induced intestinal damage is characterized by villus shortening, gross epithelial necrosis, and cellular desquamation in a murine small intestinal loop model (5). While it has also been established that CPE-induced cell death *in vitro* can be caused by classical caspase-3-dependent apo-

ptosis or by oncosis/necrosis (13), CPE-induced activation of the cell death pathway(s) *in vivo* has not been evaluated.

Therefore, an experiment tested whether CPE treatment induces intestinal caspase-3 activation in a murine small intestinal loop model of CPE disease (5). Small intestinal loops (1 per mouse) were treated with various doses (0, 25, 50, 100, or 150 μg) of CPE administered to the loops in 1 ml of Hanks' balanced salt solution (HBSS). Following a 120-min incubation, mice ($n = 10$/group) were euthanized, and the intestine was sectioned for histological evaluation and for an immunofluorescence assay (IFA) of caspase-3 activation. Specimens of small intestinal mucosa and intestinal contents were also collected from the mice for caspase-3 activity determination by colorimetric assay.

Following hematoxylin and eosin (H&E) staining, histopathology was scored according to the criteria discussed in Materials and Methods. As shown in the left panel of Fig. 1A, CPE induced significant damage in the mouse small intestinal loops. The most significant microscopic damage was seen in enterocytes, which showed different degrees of detachment from the basement membrane, pyknosis, karyorrhexis, karyolysis, cytoplasmic eosinophilia, and vacuolation. Complete loss of the epithelium was observed in the most severe cases. In addition, mucosal congestion, edema, hemorrhage, and villus blunting and fusion were also observed. The severity of overall histopathology scores correlated with increases in the CPE dose used to treat the intestinal loops (Fig. 1A and B). Minimal histologic changes developed in control (no CPE treatment) loops over the 2-h experimental duration (Fig. 1A and B).

Caspase-3 activation in the CPE-treated mouse small intestinal loops was then evaluated by colorimetric assay and immunofluorescence assay (IFA). To measure caspase-3 activation by colorimetric assay, homogenized small intestinal mucosa and intestinal contents were mixed with the caspase-3-specific substrate acetyl-Asp-Glu-Val-Asp-*p*-nitroanilide (Ac-DEVD-pNA), and, after 2 h at 37°C, absorbance in the samples was read at 405 nm. These assays detected significantly more caspase-3 activity in loops treated with $\geq$50 μg/ml of CPE than in control loops (Fig. 1C). Furthermore, the detected levels of caspase-3 activity correlated with increasing CPE doses.

Activation of caspase-3 in the CPE-treated intestinal loops was confirmed by IFA using an Alexa Fluor-594-labeled secondary antibody that detected bound primary antibody against activated caspase-3. Caspase-3 activation was then observed using confocal microscopy. When the relative amount of immunofluorescence (due to activated caspase-3) in these scans was quantified using ImageJ software, this analysis revealed that treatment with $>$50 μg/ml of CPE significantly increased caspase-3 activation over the level with the control treatment (Fig. 1D). Representative confocal microscopy images are shown in Fig. 1E. Furthermore, caspase-3 activation increased with higher CPE doses, matching the colorimetric caspase-3 activation assay results (Fig. 1C). Taken together, the results shown in Fig. 1 suggest that treatment with higher doses of CPE resulted in increased amounts of caspase-3 activation.

Time course of CPE-induced caspase-3 activation *in vivo*. Since Fig. 1 results established that CPE treatment increases intestinal caspase-3 activation in a toxin dose-responsive manner, an experiment determined the kinetics of CPE-induced caspase-3 activation in the mouse ligated intestinal loop model. For this purpose, ligated mouse small intestinal loops were treated for 0, 30, 60, 90, or 120 min with 100 μg/ml of CPE, a dose that significantly induced caspase-3 activation at 120 min, as detected by both the colorimetric and IFA assays for activated caspase-3 used for the studies represented in Fig. 1. During these time course experiments, the same assays were performed as shown in Fig. 1.

In this time course study, significant histologic damage began within 30 min in ligated mouse intestinal loops that were treated with 100 μg/ml of CPE. As evident in the H&E-stained sections, the hallmarks of damage present in these CPE-treated tissues included detachment from the basement membrane, karyopyknosis, karyorhexis, and karyolysis, in addition to hemorrhage, congestion, edema, and villus blunting (Fig. 2A).

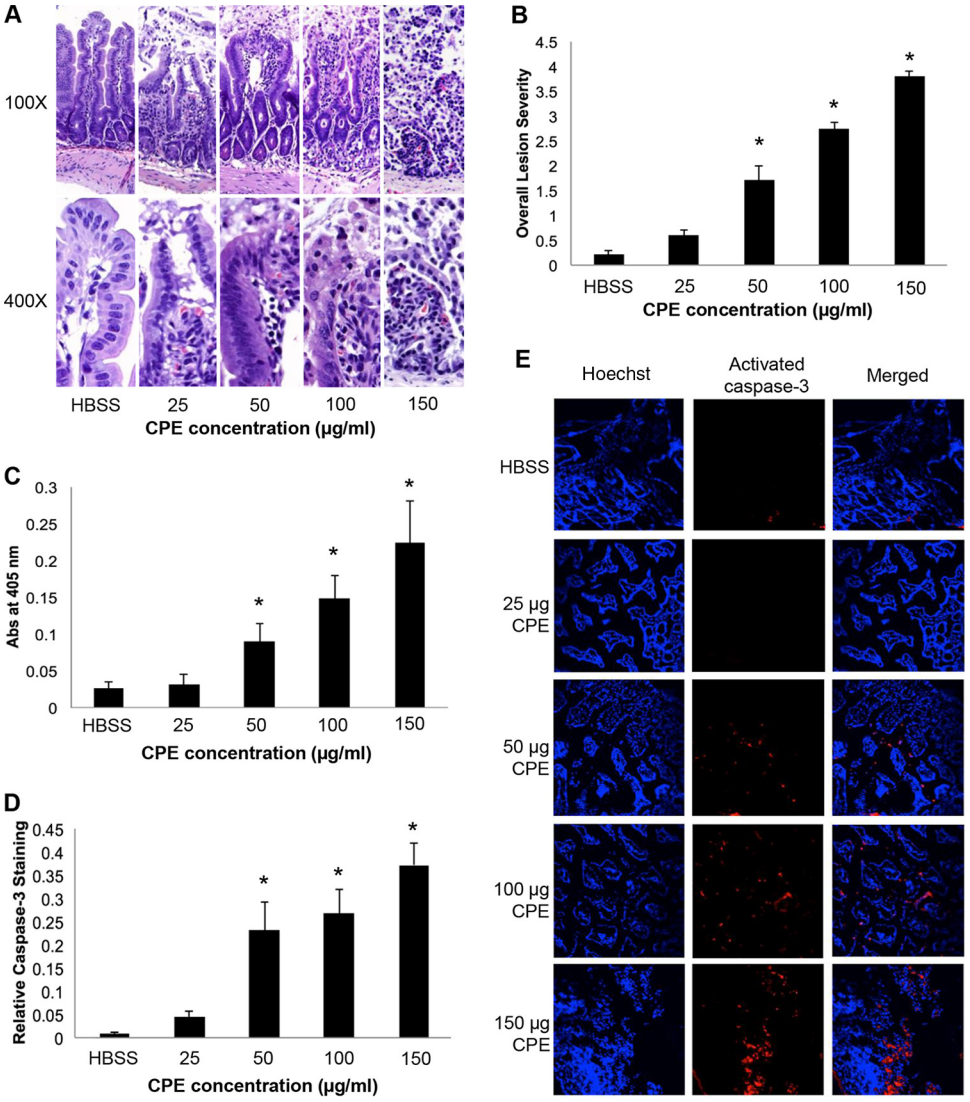

FIG 1 CPE causes intestinal damage and activates caspase-3 in the mammalian intestine in a dose-dependent manner. (A) Mouse small intestinal loops received an injection of 1 ml of HBSS containing the indicated dose of CPE for 2 h. Following cryosectioning and H&E staining, intestinal damage was observed. Abs, absorbance. (B) Histological score of intestinal loops treated with the indicated dose of CPE for 2 h. (C) Intestinal contents and mucosa from these mice were lysed and homogenized, the total protein was standardized, and caspase-3 activity was measured by colorimetric assay 2 h after the addition of Ac-DEVD-pNA. (D) Intestinal sections from this group of mice were stained by IFA for activated caspase-3. The relative amount of activated caspase-3 staining was determined using ImageJ software. (E) Representative images of IFA for activated caspase-3 (red) and epithelial nuclei stained with Hoechst 33342 (blue). Results shown in panels B to D show the means of samples from 10 mice/group. Error bars show standard errors of the means. *, $P < 0.05$.

The extent of intestinal histological damage then significantly increased with longer times of CPE treatment (Fig. 2A and B).

When caspase-3 activation in CPE-treated intestinal cell lysates was assessed by assaying cleavage of the colorimetric substrate Ac-DEVD-pNA, significant caspase-3 activity became detectable only after 90 min of CPE treatment. Caspase-3 activity then remained elevated through the 120-min duration of the assay (Fig. 2C).

Confocal immunofluorescence microscopy was also performed to detect activated caspase-3 in these CPE-treated loops. When the relative staining was calculated using ImageJ image analysis software (Fig. 2D), the analyses confirmed that caspase-3 activation was delayed until 90 min of CPE treatment in the CPE-treated loops. Representative confocal microscopy images are shown in Fig. 2E. Collectively, the results shown

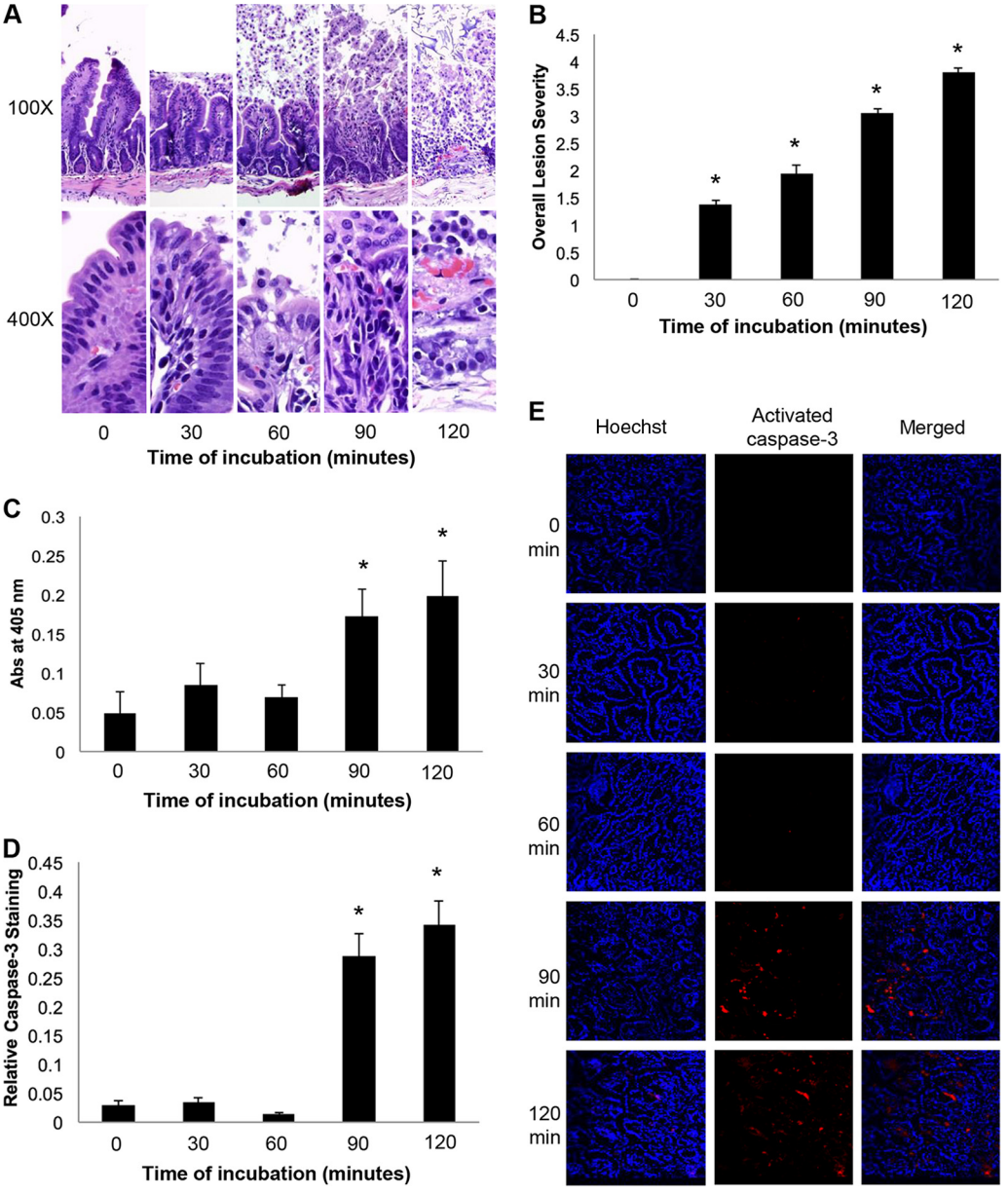

FIG 2 Time course of CPE-induced lesions and caspase-3 activation *in vivo*. (A) Mouse small intestinal loops received an injection of 1 ml of HBSS containing 100 μg of CPE for the indicated times. Following cryosectioning and H&E staining, intestinal damage was observed. (B) Histological score of intestinal loops treated with 100 μg of CPE for the indicated times. (C) Intestinal contents and mucosa from mice were lysed and homogenized, the total protein was standardized, and caspase-3 activity was measured by colorimetric assay 2 h after the addition of Ac-DEVD-pNA. (D) Intestinal sections from this group of mice were stained by IFA for activated caspase-3. The relative amount of activated caspase-3 staining was determined using ImageJ software. (E) Representative images of IFA for activated caspase-3 (red) and epithelial nuclei stained with Hoechst 33342 (blue). Results shown in panels B to D show the means of samples from 12 mice/group. Error bars show standard errors of the means. *, $P < 0.05$.

in Fig. 2 indicated that substantial caspase-3 activation occurs only after the development of histologic damage.

Caspase-3 becomes activated primarily in intestinal epithelial cells following CPE treatment of mouse small intestinal loops. With the CPE dose-response and time course experiments demonstrating that CPE activates caspase-3, an experiment evaluated which specific intestinal cells activate their caspase-3 when mouse intestinal loops are treated with CPE. For this purpose, samples of intestinal loops of mice from the time course experiment (90 and 120 min) were processed for immunohistochemistry (IHC) staining for activated caspase-3 or pan-cytokeratin (an epithelial marker [21]).

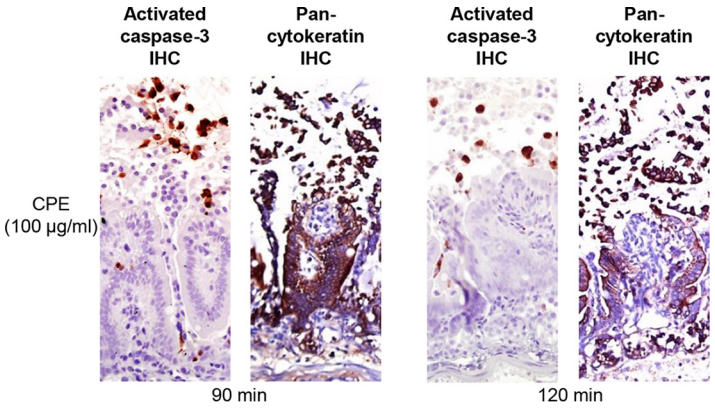

FIG 3 Caspase-3 becomes activated primarily in intestinal epithelial cells following CPE treatment of mouse small intestinal loops. Mouse small intestinal loops received an injection of 1 ml of HBSS containing 100 μg of CPE for the indicated times. IHC for activated caspase-3 and pan-cytokeratin was performed following sectioning of the tissue. Mice treated with CPE underwent significant intestinal damage, and pan-cytokeratin-stained epithelial cells along with cells stained for activated caspase-3 by IHC showed significant overlap. Images are representative of samples from 12 mice/group used in the time course experiment.

Results of this IHC staining demonstrated activated caspase-3 staining of cells in CPE-treated loops that appeared to be predominantly epithelial in nature (Fig. 3). To confirm this, IHC staining for pan-cytokeratin was performed. Pan-cytokeratin IHC staining was readily detected in the loops, and cells staining positive for activated caspase-3 were also pan-cytokeratin positive (Fig. 3). Taken together, these results indicated that the cells undergoing CPE-induced caspase-3 activation are mainly epithelial cells.

Effects of pan-caspase inhibition on CPE-induced damage in the mouse small intestine. The time course results shown in Fig. 2 suggested that caspase-3 activation may not be necessary to cause the onset of most CPE-induced intestinal damage since development of this damage preceded caspase-3 activation. To confirm this suggestion, an experiment was performed to determine whether caspase inhibition impacts the amount of intestinal damage seen in Fig. 1A and 2A. To this end, mouse intestinal loops were pretreated with Q-VD-OPh (quinolyl-valyl-O-methylaspartyl-[-2,6-difluorophenoxy]-methyl ketone), a pan-caspase inhibitor, for 15 min prior to CPE (100 μg/ml) treatment for either 90 or 120 min. At both time points, tissue sections were collected for histology and IFA staining for activated caspase-3, and small intestinal mucosa and intestinal contents were collected to measure caspase-3 activity.

In small intestinal loops treated with CPE for either 90 or 120 min, caspase-3 activation was significantly inhibited by Q-VD-OPh in comparison to activation in mice treated with CPE alone (no inhibitor). Of note, treatment with Q-VD-OPh decreased caspase-3 activation to the same levels seen in mice treated with buffer or buffer with Q-VD-OPh (no CPE). This inhibition of caspase-3 activity by Q-VD-OPh was detected using both a colorimetric assay for caspase-3 activation (Fig. 4A) and IFA image analyses (Fig. 4B).

Importantly, when loop tissue sections were H&E stained, CPE-induced intestinal damage was not inhibited by the presence of Q-VD-OPh (Fig. 4C and D). This finding indicated that activation of caspase-3, and possibly other caspases, is not required for the development of intestinal damage caused by CPE.

Caspase inhibition does not protect mice from enterotoxemic death. As mentioned in the introduction, CPE can be absorbed from the intestines to cause a fatal enterotoxemia in people with preexisting medical conditions that prolong contact of the toxin with the intestines (3, 4, 5). Since this enterotoxemia begins with contact between CPE and the intestines, an experiment evaluated whether inhibiting the activation of intestinal caspase-3 and potentially other intestinal caspases can protect mice from enterotoxemic death caused by CPE.

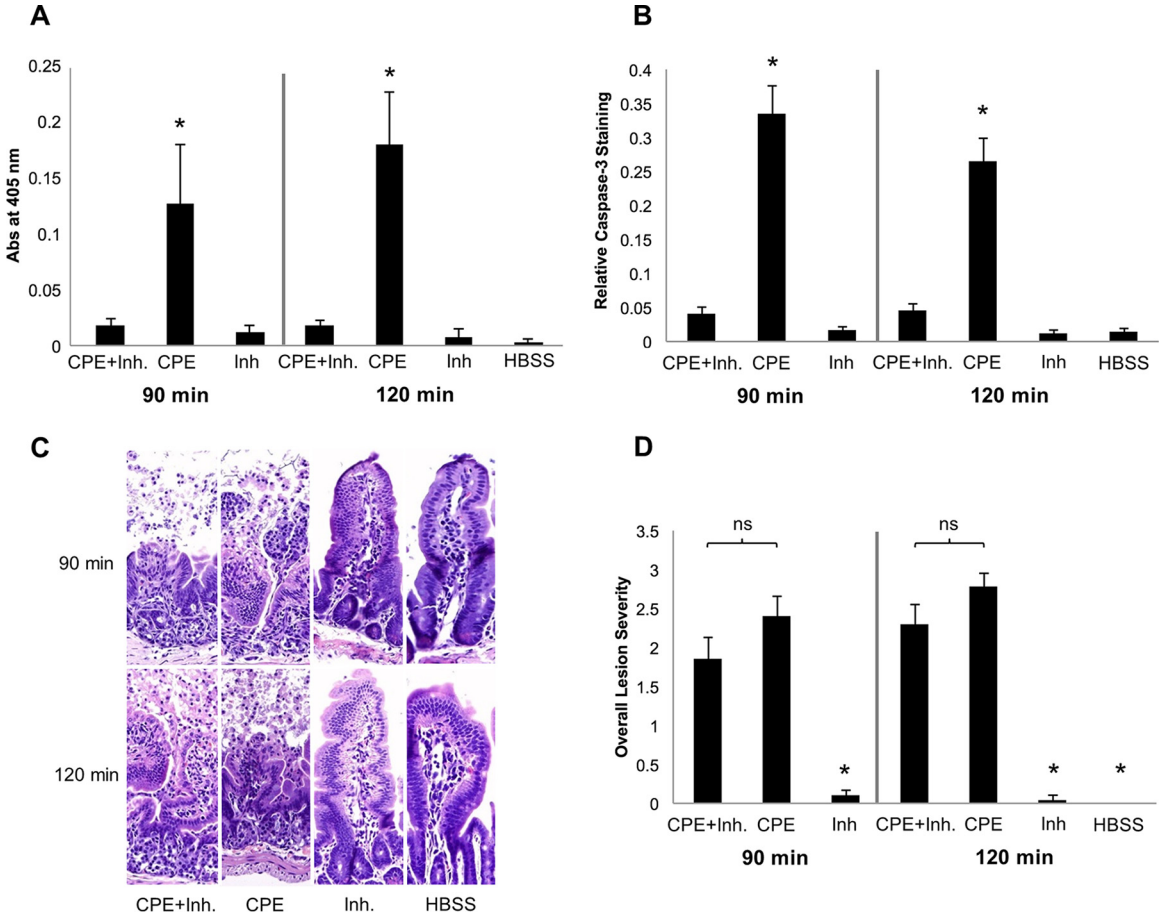

FIG 4 Caspase-3 inhibition does not protect the intestinal epithelium from CPE-induced damage. Mouse small intestinal loops received an injection of 1 ml of HBSS containing 100 μg of CPE with or without the pan-caspase inhibitor, Q-VD-OPh (Inh), for either 90 or 120 min. Mice treated with Q-VD-OPh or buffer only served as controls. (A) Intestinal contents and mucosa from the mice were lysed and homogenized, the total protein was standardized, and caspase-3 activity was measured by colorimetric assay 2 h after the addition of Ac-DEVD-pNA. (B) IFA analysis was performed to assess the amount of fluorescent staining for activated caspase-3, and ImageJ analysis was performed to determine the relative amount of caspase-3 staining. (C) Following cryosectioning and H&E staining, intestinal damage was observed. (D) Histological score of intestinal loops. Results shown in panels B to D show the means of samples from 10 mice/group. Error bars show standard errors of the means. *, $P < 0.05$; ns, not significant.

In this experiment, mice were pretreated with Q-VD-OPh prior to the addition of 100 μg/ml of CPE, and viability was monitored for up to 4 h. Analysis of intestinal samples showed that intestinal caspase-3 activity had been inhibited for the full 4-h duration of the experiment (data not shown). Damage in H&E-stained sections was similar to that described in loops of unprotected mice (see above).

All mice (100%) treated with either buffer or Q-VD-OPh alone (no CPE) survived for the full 4-h experimental period. However, when mice were treated with CPE alone, there was substantial lethality (Fig. 5). The presence of Q-VD-OPh in the intestines did not reduce CPE-induced mouse death, indicating that the inhibition of intestinal caspase-3 activation did not protect mice from death caused by CPE enterotoxemia.

The pan-caspase inhibitor Q-VD-OPh inhibits LPS-induced apoptosis of enterocytes. To demonstrate that our pan-caspase inhibitor Q-VD-OPh can block the intestinal damage caused by a substance known to activate intestinal caspase-3, we inoculated mice with lipopolysaccharide (LPS), which was previously shown to induce enterocyte apoptosis (22). As expected, LPS produced apoptosis and cell desquamation in the intestinal epithelial cells after 2 h of incubation, and the desquamated cells were positive for activate caspase-3 immunohistochemistry (data not shown); this effect was inhibited if the pan-caspase inhibitor Q-VD-OPh was injected into the intestinal loops.

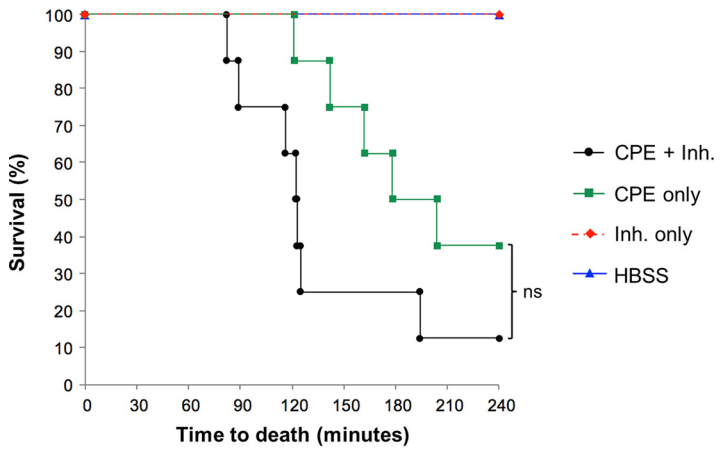

FIG 5 Caspase-3 inhibition does not inhibit enterotoxemia and murine death. Mouse small intestinal loops received an injection of 1 ml of HBSS containing 100 μg of CPE plus Q-VD-OPh (CPE + Inh), 100 μg of CPE alone, Q-VD-OPh alone (Inh), or buffer only (HBSS) for up to 4 h (8 mice/group). Mice were observed, and time to death was recorded and plotted. Kaplan-Meier survival curves were compared using log-rank analyses. A P value < 0.05 was regarded as statistically significant. ns, not significant.

DISCUSSION

A number of bacterial toxins damage the intestines. The ability of these toxins to activate cell death pathways has been well explored using *in vitro* cell culture model systems. For example, previous *in vitro* studies using CPE-treated Caco-2 cells indicated that, at a low *in vitro* CPE dose, cells undergo a cell death characteristic of caspase-3-mediated apoptosis, while high *in vitro* CPE doses caused Caco-2 cells to undergo a cell death characteristic of oncosis (13). However, the involvement of cell death pathways in bacterial toxin-induced intestinal damage has remained poorly studied. For example, while CPE can activate caspase-3 (an important contributor to some cell death pathways) in Caco-2 cells, it was not determined whether this effect occurs in the intestines or is important for CPE-induced intestinal damage. By exploring this possibility, the current study is (to our knowledge) one of the first attempts to link *in vivo* cell death-associated effects with bacterial toxin-induced intestinal damage.

When murine ligated small intestinal loops were treated, in the current study, with increasing doses of purified CPE, microscopic damage occurred in a dose-dependent manner, as noted previously (5). Also consistent with previous reports, 50 μg/ml of CPE was the minimum toxin dose required to cause tissue damage (5), which has pathophysiologic relevance since this CPE concentration lies within the range of CPE concentrations detected in feces from humans suffering food poisoning by *C. perfringens* type A enterotoxigenic strains (5, 23, 24). As also noted previously (25), CPE-induced small intestinal damage was time dependent, with significant damage observed as early as 30 min after CPE challenge. This damage began at villus tips and was mostly concentrated in enterocytes, as demonstrated by the positive staining of damaged cells by pan-cytokeratin, a universal epithelial cell marker (21).

The current study then showed, for the first time, that mice treated with increasing doses of CPE develop significant small intestinal activation of caspase-3. This activation became detectable using as little as ~50 μg of CPE/ml, and the extent of damage increased with higher toxin doses, as shown using colorimetric and IFA analyses for caspase-3 activation. Similarly, using the same assays, increased levels of caspase-3 activation were observed with longer CPE treatment times.

At least two mechanisms could be involved in CPE-induced intestinal activation of caspase-3. Our previous *in vitro* studies showed that low CPE doses induce a Ca^{+2} influx that activates calpain in Caco-2 cells (12). Calpain is known to activate caspase-3, as shown in Caco-2 cells treated with a low dose of CPE. Activated caspase-3 then leads to apoptosis, which is important for cytotoxicity under low-CPE dose treatment con-

ditions since a caspase-3 inhibitor blocked death of these Caco-2 cells (12). It is possible that CPE-induced activation of caspase-3 involves a similar pathway, particularly since previous studies showed a role for Ca^{+2} in CPE-induced intestinal damage (25). Alternatively, it is possible that CPE activates caspase-3 by a process known as anoikis, based on the following: (i) anoikis is known to activate caspase-3, (ii) anoikis develops after cells are released from basement membranes, and (iii) CPE-induced intestinal damage causes release of cells from intestinal villi. Molecular events during anoikis remain poorly defined, so it is not possible to speculate further.

However, two observations indicated that, while CPE does activate caspase-3 in the intestines, this caspase-3 activation is not necessary for the development of CPE-induced intestinal damage. First, intestinal damage was observed as early as 30 min after CPE inoculation, while significant caspase activation did not become evident until 90 min after CPE treatment. Second, when murine ligated intestinal loops were treated with both CPE and Q-VD-OPh, a broadly effective pan-caspase inhibitor, the presence of the inhibitor did not reduce intestinal damage even though it blocked intestinal caspase-3 activation.

This caspase-3-independent intestinal cell damage may be produced by other forms of cell death such as oncosis, necroptosis, autophagy, or others. Unfortunately, there are currently no good markers to study other mechanisms of cell death *in vivo*, nor are there any inhibitors or positive controls for those mechanisms of cell death in the intestines. Thus, at present we are not able to investigate further what other mechanisms of cell death were involved in the intestinal damage of our mice.

We previously demonstrated that when CPE is inoculated into intestinal loops of mice, some of this toxin is absorbed into the systemic circulation (enterotoxemia) (5), where it interacts with internal organs and causes death of mice in a dose-dependent manner. Therefore, an experiment tested whether inhibition of caspase-3 activity in the intestines, where CPE is produced during natural enterotoxemia, can affect the development of enterotoxemic lethality. When murine small intestinal loops were treated with Q-VD-OPh before challenge with CPE, this preincubation blocked the development of CPE-induced intestinal caspase-3 activation. However, lethality was not significantly different between mice treated with CPE alone or with a treatment involving the pan-caspase inhibitor Q-VD-OPh followed by CPE. These results indicate that, as also true for intestinal damage, intestinal caspase-3 activation is not essential for CPE to be absorbed from the intestine to cause enterotoxemic death. Since Q-VD-OPh is a pan-caspase inhibitor, these results may further suggest that other caspases are also not required for the development of CPE-induced intestinal damage, but this requires further verification. Additionally, it should be appreciated that the current results do not necessarily rule out intestinal caspase-3 activation, when it occurs, as possibly contributing to CPE-induced intestinal damage and or enterotoxemic death.

In addition to demonstrating that caspase-3 activation occurs in the intestine but is not necessary for CPE-induced intestinal damage or enterotoxemic death, we also looked for caspase-3 activation in liver and kidneys of mice with CPE-inoculated intestinal loops. Liver and kidney were surveyed by IFA for caspase-3 activation since both organs are known to bind CPE (5). No evidence of caspase-3 activation was observed in these organs. Whether this means that CPE activation of caspase-3 in another organ or organs does not contribute to CPE-induced enterotoxemic death is a premature conclusion since the target organs during CPE-induced enterotoxemia have not yet been identified.

A notable observation of the current study is that caspase-3 activation occurred in only certain CPE-treated intestinal epithelial cells, mostly those located in the villus tip region. Interestingly, previous studies indicated that villus tip cells also contain the greatest number of exposed CPE receptors, like claudin-4 (18). Coincident with that observation, the villus tip region is also where most CPE binds to the villus and where CPE-induced damage begins (18). Cells in the tip region are the oldest cells on the villus and, even without CPE treatment, are soon shed into the intestinal lumen, where they

then undergo caspase-3-mediated apoptosis (26, 27). As mentioned earlier, it is possible that CPE treatment accelerates this process, known as anoikis (27).

The current study shows that CPE can cause intestinal damage independently of caspase-3 activation, implying that classical caspase 3-mediated apoptosis is not required for the development of CPE-induced intestinal damage. The pathological processes responsible for the development of CPE-induced damage to intestinal regions outside the villus tip remain unresolved. One possibility is that these cells undergo direct CPE-induced necrosis, which is challenging to assess, given the absence of good *in vivo* markers for necrosis. However, this possibility appears inconsistent with previous immunohistochemical results showing limited CPE binding outside the villus tips (18). Nonetheless, it could be envisioned that prolonged contact with CPE exposes more CPE receptors on cells outside the villus to enhance their sensitivity to this toxin.

Another possible contributor to CPE-induced damage in villus regions outside the tip could involve cells dying from protein factors released by dead or dying cells at the villus tips, causing a bystander killing effect. Interestingly, such a phenomenon has been documented *in vitro* using CPE-sensitive and -resistant transfectant cells lines (20). Perhaps arguing against this possibility, it was determined that caspase-3 activation in both the sensitive and resistant cells is necessary for the development of this *in vitro* bystander killing effect (20).

Taken together, results of the current study showed that while CPE causes intestinal caspase-3 activation, the development of intestinal damage or enterotoxemia does not require intestinal caspase-3 activation. Future studies will seek to identify the role of other *in vivo* pathways involved in CPE-mediated intestinal damage.

MATERIALS AND METHODS

***Clostridium perfringens* enterotoxin.** CPE was purified to homogeneity from *C. perfringens* strain NCTC 8238 (ATCC 12916), as described previously (28).

Small intestinal loop challenge. All procedures involving animals were approved by the University of California (UC-Davis) Committee for Animal Care and Use (permit 18187). Male or female, 20- to 25-g, BALB/c mice (UC-Davis) were anesthetized by intraperitoneal administration of 0.2 ml/10 g of body weight of a mix of xylazine (0.5 mg/ml) and ketamine (5 mg/ml). Immediately before surgery, the abdomen of each mouse was disinfected with iodine solution (Betadine; Purdue Pharma LP). A midline laparotomy was performed, and an ~10- to 15-cm-long intestinal loop was prepared in the jejunum of each mouse by double ligation of the intestine without interfering with the blood supply. For each inoculation (see below), a new sterile needle and syringe were used. The incision in the peritoneum, abdominal muscles, and skin was closed in one plane using Super Glue (Henkel Corporation). This procedure was the standard for all experiments in the study.

CPE dose-response experiment. Purified CPE (25 μg, 50 μg, 100 μg, or 150 μg) dissolved in 1 ml of Hanks' balanced salt solution (HBSS) containing Ca^{2+} and Mg^{2+}, or 1 ml of control HBSS alone was injected into each loop. Mice remained under anesthesia until they were euthanized 2 h after surgery.

Time course experiment. Purified CPE (100 μg), dissolved in 1 ml of HBSS containing Ca^{2+} and Mg^{2+}, or 1 ml of HBSS alone was injected into each loop. Mice remained under anesthesia until they were euthanized at 0, 30, 60, 90, or 120 min after surgery.

Caspase inhibition. Q-VD-OPh (APExBio) (28.5 μg), a pan-caspase inhibitor, dissolved in 1 ml of HBSS, or HBSS alone was injected into each loop; 15 min later, purified CPE (100 μg), dissolved in 1 ml of HBSS containing Ca^{2+} and Mg^{2+}, or 1 ml of HBSS alone was injected into each loop. Mice were kept anesthetized until they were euthanized at 0, 30, 60, 90, or 120 min after surgery. The Q-VD-OPh concentration used was chosen to fall within the effective *in vivo* range of this compound as reported on the manufacturer's webpage.

Enterotoxemia model. To evaluate the ability of the pan-caspase inhibitor Q-VD-OPh to prevent CPE-induced lethality, the approach described above was extended to a 4-h incubation period during which death/survival was recorded. Mice were kept anesthetized until they were euthanized at the end of the 4-h treatment period unless they died spontaneously or developed severe clinical signs necessitating euthanasia. For all experiments, loop contents, mucosal scrapes, and intestinal sections were collected and then frozen at −80°C or fixed until processing for different analyses, described below.

Positive control for pan-caspase inhibitor Q-VD-OPh. To evaluate the ability of our pan-caspase inhibitor Q-VD-OPh to block the intestinal damage caused by a substance known to activate intestinal caspase-3, we inoculated mice with LPS, which was previously shown to induce enterocyte apoptosis (22). For this, Q-VD-OPh (28.5 μg), dissolved in 1 ml of HBSS, or HBSS alone was injected into ligated small intestinal loops of 8 or 6 mice, respectively, followed immediately by intraperitoneal (i.p.) injection of 10 mg/kg of LPS (Sigma). After 1.5 h of incubation the mice were euthanized, and samples of the intestinal loops were collected and processed for histopathology and caspase-3 immunohistochemistry assay. Results were assessed microscopically and scored for damage as described below for CPE-induced intestinal damage.

Histopathology. Samples of challenged intestinal loops were collected from all animals and fixed by immersion in 10% buffered formalin, pH 7.2, for 24 to 72 h. Loop sections (4 μm thick) were then prepared routinely and stained with hematoxylin and eosin (H&E). The sections were observed by a pathologist in a blinded fashion. A semiquantitative overall severity score of lesions was assigned to each section using an ordinal scale from 0 (no lesions observed) to 4 (most severe). The following criteria were considered in this score: epithelial desquamation, epithelial cell death, cell death in lamina propria, inflammation, dilation of lymphatic vessels, edema, mucus in the lumen, and villous blunting.

Colorimetric caspase-3 activity assay. Murine small intestinal mucosa and small intestinal contents were collected from all subjects at the experimental endpoint or at the time of death. Cells in the combined small intestinal mucosa/contents were lysed in lysis buffer (50 mM HEPES, pH 7.4 [Sigma-Aldrich], 0.1% 3-[(3-cholamidopropyl)-dimethylammonio]-1-propanesulfonate [CHAPS; Sigma-Aldrich], 1 mM dithiothreitol [Fisher Scientific], 0.1 mM EDTA [Fisher Scientific]) (12) using a Dounce homogenizer. Cell debris was then pelleted by centrifugation at 14,000 rpm for 10 min at 4°C, and the soluble fraction was used for the assay. The total protein concentration of the cell lysates was determined using a Pierce bicinchoninic acid (BCA) protein assay kit (Thermo Scientific), and proteins were diluted to a final concentration of 100 μg/100 μl in assay buffer, with a final concentration of 50 mM HEPES, pH 7.4, 100 mM NaCl, 0.1% CHAPS, 10 mM dithiothreitol, 1 mM EDTA, and 10% glycerol (12). Caspase-3 substrate, Ac-DEVD-*p*-nitroanilide (Ac-DEVD-pNA; Sigma-Aldrich), was added to a final concentration of 4 mM, and samples were then incubated in the dark for 2 h at 37°C. The absorbance at 405 nm was then quantified using a BioTek Synergy plate reader. The sensitivity of the colorimetric assay was evaluated *in vitro*. When 10 U, 5 U, and 3 U of activated caspase-3 (BioVision) were tested, 10 U (~83 ng) was the minimum amount of active caspase-3 that this assay was able to detect. Therefore, this assay is sensitive to between 40 and 80 ng of active caspase-3.

Immunofluorescence assay for activated caspase-3. Thin sections of each challenged loop were immediately embedded in a 22-oxacalcitriol (OCT) freezing compound (Tissue Tech, St. Laurent, Quebec, Canada) and frozen at −80°C until processed by an activated caspase-3 immunofluorescence assay. Briefly, 4-μm-thick sections were cut in a cryostat and mounted on glass slides. Prepared slides were thawed to room temperature and fixed with 4% paraformaldehyde (Fisher Scientific) for 10 min at room temperature and washed three times with phosphate-buffered saline (PBS). The slides were then blocked and permeabilized for 30 min at room temperature in PBS containing 5% goat serum (Fisher Scientific) and 0.1% Triton X-100, followed by another three washes with PBS. Primary antibody specific for activated caspase-3 (ASP175; Cell Signaling Technology) was incubated on the slides for 2 h at room temperature, followed by three PBS washes. Alexa Fluor 594-conjugated goat anti-rabbit IgG antibody (Invitrogen Molecular Probes) was incubated with the slides for 1 h at room temperature, followed by staining with Hoechst 33342 (Invitrogen) for 10 min. After three PBS washes, slides were mounted with Aqua Poly/Mount (Polysciences, Inc.) with glass coverslips and stored at 4°C until images were obtained on a FluoView FV1000 Olympus confocal laser scanning microscope with FV10-ASW (version 1.4) software at a magnification of ×200. Mean pixel intensity for activated caspase-3- and Hoechst 33342-stained nuclei was determined for each cell using ImageJ software (29) to determine the relative amount of staining for activated caspase-3/cell/20× field.

IHC detection of activated caspase 3 and pan-cytokeratin. Tissue sections from challenged small intestinal loops from the time course experiment were processed for immunohistochemistry (IHC) according to standard operational procedures of the California Animal Health and Food Safety Laboratory System (activated caspase-3) and the Veterinary Medical Teaching Hospital (pan-cytokeratin), both at UC-Davis. Briefly, for activated caspase-3 IHC detection, a Dako EnVision kit (Dako, Carpenteria, CA) was employed according to the instructions of the manufacturer. A rabbit polyclonal anti-activated caspase-3 (ASP175; Cell Signaling Technology) was used at a 1:100 dilution. The immunoreactivity was visualized with Vector NovaRED chromogen. A lymph node from a cow with lymphoma (a tissue in which there is abundant apoptosis) and small intestine of mice treated with LPS were employed as positive controls. Sections of lymph node from a normal cow and tissues in which the primary antibody was replaced by normal rabbit serum were used as negative controls. For pan-cytokeratin IHC detection, tissue sections were incubated with a 3% solution of hydrogen peroxide to block endogenous peroxidase, followed by antigen retrieval with proteinase K. Nonspecific binding was blocked by treating the samples with normal horse serum blocking solution, followed by incubation with a mouse anti-pan-cytokeratin antibody (Lu-5) (CM043C; BioCare) at a 1:100 dilution. Sections were then incubated with BioCare mouse-on-canine horseradish peroxidase (HRP) polymer. The immunoreactivity was visualized with Vector NovaRED chromogen. Sections of colon and skin were used as positive controls. Tissues incubated with normal serum or PBS instead of the primary antibodies were used as negative controls.

Statistical analyses. Statistical analyses were performed using R for Mac (version 3.3.1). The Shapiro-Wilk and Anderson-Darling tests were used to assess for normal distribution of data. When the criterion of normality was met, groups were compared by one-way analysis of variance (ANOVA), followed by Tukey's test for multiple comparisons as *post hoc* analysis. In the case of nonnormally distributed data, a nonparametric Kruskal-Wallis test was used, followed by Dunn's test as *post hoc* analysis. Kaplan-Meier survival curves were compared using log rank analyses. In all cases, a P value of <0.05 was regarded as statistically significant. For dose-response experiments, mouse histology and caspase-3 activity (colorimetric and IFA) were performed for a total of 10 mice/group. For the time course experiments, mouse histology and caspase-3 activity (colorimetric and IFA) were performed for a total of 12 mice/group. For inhibitor studies assessing histologic damage and caspase-3 activity, 10 mice/group were used. In the enterotoxemia experiment, a total of 8 mice/group were utilized.

ACKNOWLEDGMENTS

This research was generously supported by grant AI0198844-35 (to B.A.M.) from the National Institute of Allergy and Infectious Diseases.

The content is solely the responsibility of the authors and does not necessarily represent the official views of the National Institutes of Health.

REFERENCES

1. Abrahao C, Carman RJ, Hahn H, Liesenfeld O. 2001. Similar frequency of detection of *Clostridium perfringens* enterotoxin and *Clostridium difficile* toxins in patients with antibiotic-associated diarrhea. Eur J Clin Microbiol Infect Dis 20:676–677.
2. Carman RJ. 1997. *Clostridium perfringens* in spontaneous and antibiotic-associated diarrhea of man and other animals. Rev Med Microbiol 8(Suppl 1):S43–S46. https://doi.org/10.1097/00013542-199712001-00023.
3. Centers for Disease Control and Prevention. 2012. Fatal foodborne *Clostridium perfringens* illness at a state psychiatric hospital—Louisiana, 2010. MMWR Morb Mortal Wkly Rep 61:605–608.
4. Bos J, Smithee L, McClane BA, Distefano RF, Uzal F, Songer JG, Mallonee S, Crutcher JM. 2005. Fatal necrotizing colitis following a foodborne outbreak of enterotoxigenic *Clostridium perfringens* type A infection. Clin Infect Dis 40:e78–e83. https://doi.org/10.1086/429829.
5. Caserta JA, Robertson SL, Saputo J, Shrestha A, McClane BA, Uzal FA. 2011. Development and application of a mouse intestinal loop model to study the in vivo action of *Clostridium perfringens* enterotoxin. Infect Immun 79:3020–3027. https://doi.org/10.1128/IAI.01342-10.
6. McClane BA, Robertson SL, Li J. 2013. *Clostridium perfringens*, p 465–489. *In* Doyle MP, Buchanan RL (ed), Food microbiology: fundamentals and frontiers, 4th ed. ASM Press Washington, DC.
7. Freedman JC, Shrestha A, McClane BA. 2016. *Clostridium perfringens* enterotoxin: action, genetics, and translational applications. Toxins (Basel) 8:E73. https://doi.org/10.3390/toxins8030073.
8. Chen J, Theoret JR, Shrestha A, Smedley JG, III, McClane BA. 2012. Cysteine-scanning mutagenesis supports the importance of *Clostridium perfringens* enterotoxin amino acids 80 to 106 for membrane insertion and pore formation. Infect Immun 80:4078–4088. https://doi.org/10.1128/IAI.00069-12.
9. Robertson SL, Smedley JG, III, Singh U, Chakrabarti G, Van Itallie CM, Anderson JM, McClane BA. 2007. Compositional and stoichiometric analysis of *Clostridium perfringens* enterotoxin complexes in Caco-2 cells and claudin 4 fibroblast transfectants. Cell Microbiol 9:2734–2755. https://doi.org/10.1111/j.1462-5822.2007.00994.x.
10. Matsuda M, Sugimoto N. 1979. Calcium-independent and dependent steps in action of *Clostridium perfringens* enterotoxin on HeLa and Vero cells. Biochem Biophys Res Commun 91:629–636. https://doi.org/10.1016/0006-291X(79)91568-7.
11. McClane BA, Wnek AP, Hulkower KI, Hanna PC. 1988. Divalent cation involvement in the action of *Clostridium perfringens* type A enterotoxin. Early events in enterotoxin action are divalent cation-independent. J Biol Chem 263:2423–2435.
12. Chakrabarti G, McClane BA. 2005. The importance of calcium influx, calpain and calmodulin for the activation of CaCo-2 cell death pathways by *Clostridium perfringens* enterotoxin. Cell Microbiol 7:129–146. https://doi.org/10.1111/j.1462-5822.2004.00442.x.
13. Chakrabarti G, Zhou X, McClane BA. 2003. Death pathways activated in CaCo-2 cells by *Clostridium perfringens* enterotoxin. Infect Immun 71:4260–4270. https://doi.org/10.1128/IAI.71.8.4260-4270.2003.
14. Hidalgo IJ, Raub TJ, Borchardt RT. 1989. Characterization of the human colon carcinoma cell line (Caco-2) as a model system for intestinal epithelial permeability. Gastroenterology 96:736–749. https://doi.org/10.1016/S0016-5085(89)80072-1.
15. Rousset M, Chevalier G, Rousset JP, Dussaulx E, Zweibaum A. 1979. Presence and cell growth-related variations of glycogen in human colorectal adenocarcinoma cell lines in culture. Cancer Res 39:531–534.
16. Wikman A, Karlsson J, Carlstedt I, Artursson P. 1993. A drug absorption model based on the mucus layer producing human intestinal goblet cell line HT29-H. Pharm Res 10:843–852. https://doi.org/10.1023/A:1018905109971.
17. Gill N, Wlodarska M, Finlay BB. 2011. Roadblocks in the gut: barriers to enteric infection. Cell Microbiol 13:660–669. https://doi.org/10.1111/j.1462-5822.2011.01578.x.
18. Smedley JG, III, Saputo J, Parker JC, Fernandez-Miyakawa ME, Robertson SL, McClane BA, Uzal FA. 2008. Noncytotoxic *Clostridium perfringens* enterotoxin (CPE) variants localize CPE intestinal binding and demonstrate a relationship between CPE-induced cytotoxicity and enterotoxicity. Infect Immun 76:3793–3800. https://doi.org/10.1128/IAI.00460-08.
19. Shrestha A, McClane BA. 2015. *Clostridium perfringens* enterotoxin, p 815–838. *In* Alouf J, Ladant D, Popoff M (ed), The comprehensive sourcebook of bacterial protein toxins, 4th ed. Elsevier, Amsterdam, Netherlands.
20. Shrestha A, Hendricks MR, Bomberger JM, McClane BA. 2016. Bystander host cell killing effects of *Clostridium perfringens* enterotoxin. mBio 7:e02015-16. https://doi.org/10.1128/mBio.02015-16.
21. Paladino G, Marino C, La Terra Mule S, Civiale C, Rusciano D, Enea V. 2004. Cytokeratin expression in primary epithelial cell culture from bovine conjunctiva. Tissue Cell 36:323–332. https://doi.org/10.1016/j.tice.2004.05.003.
22. Williams JM, Duckworth CA, Watson AJ, Frey MR, Miguel JC, Burkitt MD, Sutton R, Hughes KR, Hall LJ, Caamano JH, Campbell BJ, Pritchard DM. 2013. A mouse model of pathological small intestinal epithelial cell apoptosis and shedding induced by systemic administration of lipopolysaccharide. Dis Model Mech 6:1388–1399. https://doi.org/10.1242/dmm.013284.
23. Berry PR, Rodhouse JC, Hughes S, Bartholomew BA, Gilbert RJ. 1988. Evaluation of ELISA, RPLA, and Vero cell assays for detecting Clostridium perfringens enterotoxin in faecal specimens. J Clin Pathol 41:458–461. https://doi.org/10.1136/jcp.41.4.458.
24. Bartholomew BA, Stringer MF, Watson GN, Gilbert RJ. 1985. Development and application of an enzyme linked immunosorbent assay for *Clostridium perfringens* type A enterotoxin. J Clin Pathol 38:222–228. https://doi.org/10.1136/jcp.38.2.222.
25. Sherman S, Klein E, McClane BA. 1994. *Clostridium perfringens* type A enterotoxin induces tissue damage and fluid accumulation in rabbit ileum. J Diarrhoeal Dis Res 12:200–207.
26. Grossmann J, Walther K, Artinger M, Rummele P, Woenckhaus M, Scholmerich J. 2002. Induction of apoptosis before shedding of human intestinal epithelial cells. Am J Gastroenterol 97:1421–1428. https://doi.org/10.1111/j.1572-0241.2002.05787.x.
27. Bertrand K. 2011. Survival of exfoliated epithelial cells: a delicate balance between anoikis and apoptosis. J Biomed Biotechnol 2011:534139. https://doi.org/10.1155/2011/534139.
28. Freedman JC, Hendricks MR, McClane BA. 2017. The potential therapeutic agent mepacrine protects Caco-2 cells against *Clostridium perfringens* enterotoxin action. mSphere 2:00352–17. https://doi.org/10.1128/mSphere.00352-17.
29. Schneider CA, Rasband WS, Eliceiri KW. 2012. NIH Image to ImageJ: 25 years of image analysis. Nat Methods 9:671–675. https://doi.org/10.1038/nmeth.2089.